SAND REPORT

Effect of high-viscosity interphases on drainage between hydrophilic surfaces

Peter J. Feibelman

Sandia National Laboratories

Effect of high-viscosity interphases on drainage between hydrophilic surfaces

Peter J. Feibelman
Surface and Interface Sciences Department

Sandia National Laboratories
P.O. Box 5800
Albuquerque, NM 87185-1415

Abstract

Drainage of water from the region between an advancing probe tip and a flat sample is reconsidered under the assumption that the tip and sample surfaces are both coated by a thin water "interphase" (of width ~a few nm) whose viscosity is much higher than the bulk liquid's. A formula derived by solving the Navier-Stokes equations allows one to extract an interphase viscosity of ~59 KPa-sec (or ~6.6×10^7 times the viscosity of bulk water at 25C) from Interfacial Force Microscope measurements with both tip and sample functionalized hydrophilic by OH-terminated tri(ethylene glycol) undecylthiol, self-assembled monolayers.

Introduction –

Surprisingly long-ranged "hydration forces" observed between solids separated by water are thought to result from the formation of nm scale, structured-liquid surface coatings or *interphases*.[1] Hydrophobic solids mutually attract, for example, expelling several nm of water between them. This remarkable phenomenon is attributed to low-density or gaseous interphase formation at hydrophobic surfaces.[2] Hydrophilic surfaces experience *repulsive* hydration forces, but the nature of their interphases is less well established. They may[1] or may not[3] be denser than bulk water and their viscosity may or may not be greater, or even much greater.[4,5] Deepening our understanding of water interphases is important because of their biological and geophysical implications, and their potential importance in nanofluidic technologies.

Kim, Kushmerick, Houston and Bunker's (KKHB's)[6] Interfacial Force Microscope (IFM)[7] measurements of viscous drag on a hydrophilic probe tip approaching a hydrophilic surface in water provide an example where dissipation in water adjacent to a hydrophilic surface appears to be unusually strong, perhaps indicating the formation of "solid-like" or "slushy" interphases. With both the Au sample and the IFM's Au tip functionalized by OH-terminated tri(ethylene glycol) undecylthiol [or "EG3OH"] self-assembled monolayers, KKHB report that within about 5 nm of contact, energy dissipation in water is strongly dependent on tip speed. According to their quantitative analysis, *the data imply an interphase viscosity that is a factor of ~10^6 larger than the viscosity of bulk water.*[6]

This conclusion, however, is based on a somewhat *ad hoc* generalization of Chan & Horn's (CH's) hydrodynamic theory of drainage of a liquid thin film from between two approaching solids.[8] The purpose of the present work is to place the required generalization on a firm footing, and then to revisit the application of theory to KKHB's data. The result appears to confirm the applicability of bulk hydrodynamics to KKHB's drainage experiment, but also points to a need for higher quality data.

CH's derivation (an application of Reynolds' theory of lubrication[9]) yields a repulsive hydration force $6\pi\eta R^2 v/D$, at tip-sample separation, D, and approach velocity, v, for a tip whose radius of curvature is R, in a liquid of viscosity, η. This force-law, however, is incapable of describing KKHB's result (see Fig. 1) that the IFM tip only experiences a large force within ~5 nm of the sample surface, and is much smaller outside that range. KKHB viewed the short-range repulsion as a

direct manifestation of thin, viscous interphases, on tip and sample, and guessed that the cutoff of the hydration force at $D_0 \sim$ 5nm could be adequately represented by modifying the CH force law to $6\pi\eta R^2 v(1 - D/D_0)/D$. Deciding whether this guess is correct is the first objective of the present work. That it might *not* be is suggested by the fit in Fig. 2, reproduced from Ref. 6, Fig. 5. In this figure, the raw data of Fig. 1 has been corrected for the compliances of the EG3OH SAM's and the Au tip and sample (see Ref. 6, for an explanation of how), and the resulting hydration force fitted to $6\pi\eta R^2 v(1 - D/D_0)/D$. Notice that the curvature of the data is not well described by the theoretical, solid curves. An improved theoretical discussion is therefore warranted. This is the subject of the next sections of this article. It yields a simple modification of the force formula KKHB used, to $6\pi\eta R^2 v (1 - D/D_0)^2/D$.

Fig. 3 shows that this corrected force formula allows much better fits to the IFM force vs. separation data, and thus, yields an improved (and actually, a considerably increased) estimate of the interphase viscosity. However, closer examination of the figure makes plain that the measured forces for different speeds vanish at different relative displacements. This is a problem, because in the drainage theory, the hydration force scales directly with tip speed. Therefore the displacement at which the force reaches zero ought to be the same *for all speeds.*

More data is wanted, accordingly, to determine the source of the discrepancy, for example to learn if inhomogeneity of the self-assembled monolayers coating the tip and sample is the key problem. Measurements at more than just two approach speeds would also be welcome.

Hydration force for drainage with a spatially-varying viscosity -
To analyze KKHB's results quantitatively, one must derive a force vs. separation formula appropriate to the circumstance that fluid viscosity is not constant, but dependent on distance from sample or tip (specifically, higher in the slushy surface coatings than in bulk water). Such a formula is implicit in the "modified Reynolds equation" developed by Tichy[10] to deal with lubrication when asperities on opposing, functionalized surfaces overlap. One is derived explicitly in this note through a straightforward elaboration beyond the assumption of a spatially *invariant* viscosity of Chan and Horn's (CH's) thin-film "drainage" theory.[8] Application of the new derivation to the IFM data[6] requires an upward revision (by a factor of 33) of KKHB's estimated interphase viscosity, to ~59 KPa-sec, or 6.6×10^7 times the viscosity of bulk water at 25C.[11]

The lubrication approximation –
CH applied the "lubrication approximation" to the Navier-Stokes (NS) equations to the motion of a curved surface toward a planar one.[8] They assumed both surfaces to be rigid and the fluid to have a *constant* viscosity. In what follows, allowing for a spatially-varying viscosity, I derive general asymptotic results applicable to a tip nearly at contact with the planar sample and to a separation such that the slushy coatings barely touch. In addition, for a simple model – a step-function change in viscosity at the interphase boundary – I arrive at an explicit formula for the hydrodynamic force on a tip.

The lubrication approximation is defined by the following assumptions:[8,9] 1) fluid velocities are sufficiently small that terms in the N-S equation quadratic in velocities can be ignored, 2) the fluid velocity normal to the plane surface (henceforth, the z-direction) is small compared to the velocity parallel to it, 3) the x and y variation of the velocity parallel to the plane surface (which by convention lies in an x-y plane) is weak compared to its variation along z, and 4) the pressure gradient along z is negligible. In addition, for the analysis of KKHB's data,[6] the radius of curvature of the curved (i.e., the tip) surface is taken to be large compared to the distance between it and the plane surface and the viscosity is presumed to be a function only of the distance from either surface. Beyond the lubrication approximation, I also require in what follows that the fluid flow be steady-state, i.e., all velocities are constant in time.

For hydrophilic surfaces, it is reasonable to impose "stick" boundary conditions at each surface, i.e., to require the parallel component of the fluid velocity to vanish there. Because of the large radius of curvature of the curved surface, this boundary condition may be applied to the velocity components in the x- and y-directions, even though the tangent to the curved surface necessarily has a small z-component. Similarly, one may ignore x- and y-derivatives of the viscosity that are non-zero because its interphase conforms to the curved surface.

General Derivation of Drainage Formulas –
Given these considerations, the momentum equation for fluid flow, as the curved surface approaches the planar surface, is,[8]

$$\frac{\partial}{\partial z}\left(\eta(z)\frac{\partial}{\partial z}\right)\vec{v}_T = \vec{\nabla}_T P \qquad , \qquad (1)$$

where $\eta(z)$ is the spatially varying viscosity, $\vec{v}_T(z)$ is the parallel velocity of the fluid and $P(z)$ is the fluid pressure. Eq. 1 integrates to yield an explicit, general result,

$$\vec{v}_T(z) = \int_{C_1}^{z} dz'(z' - C_2) / \eta(z') \vec{\nabla}_T P \quad , \tag{2}$$

where C_1 and C_2 are constants of integration to be determined by applying boundary conditions. Let the planar surface lie at z=0. Then one can satisfy the stick boundary condition there, $\vec{v}_T(0) = 0$, by setting $C_1=0$. Supposing the curved surface to lie at z=H(x,y) [or z=H(r) for a cylindrically symmetric tip], one finds that,

$$C_2 = \frac{\int_0^H zdz / \eta(z)}{\int_0^H dz / \eta(z)} \quad , \tag{3}$$

by applying the second stick boundary condition, $\vec{v}_T(H) = 0$. Note that if the upper and lower surfaces are of identical material and structure, then Eq. 3 yields $C_2 = H/2$, by symmetry. More generally, C_2 is the center of gravity of the inverse viscosity, which I henceforth call $\overline{Z}(x, y)$.

Following Chan & Horn,[8] I now integrate the continuity equation,

$$\frac{\partial v_z}{\partial z} = -\vec{\nabla}_T \cdot \vec{v}_T(z) \quad , \tag{4}$$

(wherein the subscript T stands for "transverse," i.e. x- and y-derivatives only). Once again applying the stick boundary condition at z=0, this yields,

$$v_z(z) = -\vec{\nabla}_T \cdot \int_0^z dz' \int_0^{z'} dz'' \frac{(z'' - \overline{Z}(x, y))}{\eta(z'')} \vec{\nabla}_T P \quad , \tag{5}$$

or, interchanging the order of z' and z" integration,

6

$$v_z(z) = -\vec{\nabla}_T \cdot \int_0^z dz' \frac{\left(z' - \bar{Z}(x,y)\right)(z-z')}{\eta(z')} \vec{\nabla}_T P \quad . \tag{6}$$

At z=H, the z-component of the fluid velocity must equal the velocity of the curved surface. Specializing to the case in which the curved surface is that of a parabolic cylindrical tip, whose curvature radius is R and whose apex lies a distance D above the planar surface, one has,

$$H(x,y) = H(r) = D + r^2/2R \tag{7}$$

near the tip apex, where $r^2 = x^2 + y^2$. In consequence, $\bar{Z}(x,y) = \bar{Z}(r)$, and, equating the tip speed, *dD/dt* with the normal velocity of the fluid at the tip surface, $v_z(H)$, Eq. 6 simplifies to,

$$\frac{dD}{dt} = \frac{\left(H - \bar{Z}\right)^2}{\eta(H)} \frac{dH}{dr} \frac{dP}{dr} + \int_0^H dz \frac{\left(z^2 - \bar{Z}^2\right)}{\eta(z)} \frac{1}{r} \frac{d}{dr}\left(r\frac{dP}{dr}\right) \quad . \tag{8}$$

The two terms on the right-hand-side of Eq. 8 combine, using the definition of $\bar{Z}$ in Eq. 3, to give,

$$\frac{dD}{dt} = \frac{1}{r}\frac{d}{dr}\left(rg(r)\frac{dP}{dr}\right) \quad , \tag{9}$$

where g(r) is defined by,

$$g(r) \equiv \int_0^{H(r)} dz \frac{\left(z^2 - \bar{Z}^2(r)\right)}{\eta(z)} \quad . \tag{10}$$

Eq. 9 is a differential equation for *P(r)*, which, applying the boundary condition that *P(0)* be finite, has the solution,

$$P(r) = -\int_r^\infty dr' \frac{r'}{2g(r')} \frac{dD}{dt} + P(\infty) \quad . \tag{11}$$

From Eq. 11, the dissipative hydrodynamic force in the normal direction can be obtained as the integral of the stress over the plane surface according to (see Ref. 8),

$$F_H = \int d^2 r \left(P(r) - P(\infty) - 2\eta \frac{\partial v_z}{\partial z} \right)_{z=0} \qquad . \qquad (12)$$

The last term in the integrand vanishes, according to Eq. 5. (This is a consequence of the stick boundary condition at the sample surface and the equation of continuity.) Thus, substituting Eq. 11 into Eq. 12, one obtains the general formula for the force,

$$F_H = -\frac{\pi}{2} \int_0^\infty dr \frac{r^3}{g(r)} \frac{dD}{dt} \qquad . \qquad (13)$$

In the next section, I evaluate this expression for F_H, the quantity KKHB measured, given simple model assumptions.

Hydration force for a step-function model viscosity –
To begin, because KKHB's tip and sample surface were chemically identical (EG3OH-coated Au), the viscosity must have been symmetric. That is,

$$\eta(z) = \eta(H - z) \qquad . \qquad (14)$$

This symmetry means (cf. above) that $\overline{Z} = H/2$ and it allows Eq. 10 to be rewritten as,

$$g(r) = 2 \int_0^{H(r)/2} dz \frac{(z - H(r)/2)^2}{\eta(z)} \qquad . \qquad (15)$$

To proceed farther, one needs a model viscosity function. The simplest[6] corresponds to the assumption that the viscosity is large and equal to η_s (s for "slush") if the argument of η is between 0 and w, and equal to η_w (w for "water") if it lies between w and $H(s)/2$. This corresponds to the schematic of Fig. 4. Notice in

the figure that pure "slush" occupies a cylinder surrounding the tip apex (at $r=0$) *if D is small enough*. How small does it have to be? Evidently, D must be smaller than *2w*, so that the tip and sample slush regions overlap. This being the case, the pure slush cylinder radius is given by $D - w + r^2/2R = w$, or $r^2 = 2R\,(2w - D)$. Thus the *s*-integral of Eq. 13 should be written as

$$F_H = -\frac{\pi}{2} \int_0^{\sqrt{2R(2w-D)}} dr \, \frac{r^3}{g(r)} \frac{dD}{dt} - \frac{\pi}{2} \int_{\sqrt{2R(2w-D)}}^{\infty} dr \, \frac{r^3}{g(r)} \qquad . \qquad (16)$$

In the first term, since there is pure slush over the entire range of *z*, I obtain for *g(r)*,

$$g(r) = H^3(r)/12\eta_s \qquad . \qquad (17)$$

In the second term, the z-integral covers both slush and bulk water regions, and *g(r)* is instead,

$$g(r) = (1/\eta_s) \int_0^w dz (H(r)/2 - z)^2 + (1/\eta_w) \int_w^{H(r)/2} dz (H(r)/2 - z)^2 \quad . \quad (18)$$

What is interesting and important about this result is that if $\eta_w \ll \eta_s$, then the second term on the right hand side of Eq. 18 dominates the first. This makes the second term on the right hand side of Eq. 16 small. Thus, the pure slush cylinder dominates the value of F_H.

Because it is important for estimating the leading contribution of η_w to F_H, I temporarily retain all contributions to *g(r)*. Thus, Eq. 18 yields,

$$g(r) = (1/3\eta_s)\{[H(r)/2]^3 - [H(r)/2 - w]^3\} + (1/3\eta_w)[H(r)/2 - w]^3 .$$
(19)

Now I evaluate the right-hand-side of Eq. 16, starting with the easy first term. Substituting from Eqs. 7 and 17, it takes the form

$$F_H{}^{(c)} = -6\pi\eta_s \frac{dD}{dt} \int_0^{\sqrt{2R(2w-D)}} dr \frac{r^3}{(D+r^2/2R)^3} \quad , \quad (20)$$

where the superscript "c" is a reminder that this term comes from the "cylinder" of pure slush. The integral can be performed trivially, yielding,

$$F_H{}^{(c)} = -6\pi\eta_s \frac{R^2}{D} \frac{dD}{dt} \left(1 - \frac{D}{2w}\right)^2 \quad , \quad (21)$$

which is CH's formula times a quadratic cutoff as $D \to 2w$. This cylinder term, as noted above, is the dominant contribution to the hydrodynamic dissipative force in the limit $\eta_w << \eta_s$.

To estimate the contribution of the second term on the right hand side of Eq. 16 (with superscript "oc" for "outside the cylinder"), I substitute from Eq. 19 for $g(r)$. The result is that,

$$F_H{}^{(oc)} = -6\pi\eta_w \frac{dD}{dt} \int_{\sqrt{2R(2w-D)}}^\infty dr \frac{r^3}{\rho(D+r^2/2R)^3 + (1-\rho)(D+r^2/2R - 2w)^3}$$
, (22)

where $\rho \equiv \eta_w / \eta_s$. To evaluate the integral of Eq. 22 to leading order in the limit $\rho \to 0$ requires some analysis. The reason is that for $\rho = 0$, the integrand diverges strongly at the lower integration limit, which invalidates a Taylor expansion in ρ. To proceed, then, let

$$r^2/4R = x + w - \frac{D}{2} \quad . \quad (23)$$

Substituting this variable change into Eq. 22, implies that,

$$F_H{}^{(oc)} = -6\pi\eta_w R^2 \frac{dD}{dt} \int_0^\infty dx \frac{x + w - \dfrac{D}{2}}{\rho(w+x)^3 + (1-\rho)x^3} \quad . \quad (24)$$

For the sake of approaching the limit $\rho \to 0$, I now make the further variable change, $x = \rho^{1/3} w \sigma$, yielding,

$$F_H^{(oc)} = -6\pi\eta_w R^2 \frac{dD}{dt} \int_0^\infty \rho^{1/3} w \, d\sigma \frac{\rho^{1/3} w \sigma + w - \dfrac{D}{2}}{\rho w^3 (1 + \sigma^3) + 3\rho^{4/3} w^3 \sigma + 3\rho^{5/3} w^3 \sigma^2} \quad .$$

(25)

This formula allows one to factor a ρ out of the denominator and then let ρ approach zero. The result, recalling the definition, $\rho \equiv \eta_w / \eta_s$, is that to leading order in the small water viscosity,

$$F_H^{(oc)} = -\frac{4\pi^2}{3\sqrt{3}} \eta_w^{1/3} \eta_s^{2/3} \frac{R^2}{w} \frac{dD}{dt}\left(1 - \frac{D}{2w}\right) \quad . \tag{26}$$

Collecting terms, one learns, finally, that if the slush viscosity is much bigger than that of bulk water, then,

$$F_H = -6\pi\eta_s \frac{R^2}{D} \frac{dD}{dt}\left(1 - \frac{D}{2w}\right)^2 - \frac{4\pi^2}{3\sqrt{3}} \eta_w^{1/3} \eta_s^{2/3} \frac{R^2}{w} \frac{dD}{dt}\left(1 - \frac{D}{2w}\right) \quad .$$

(27)

In the KKHB's experiments,[2] with $\eta_w / \eta_s \sim 10^{-6}$, the second term is negligible, other than very close to D=2w.

Asymptotic results for the hydration force –
Before leaving the force formula of Eq. 27, it is important to see why the dominant first term vanishes quadratically, i.e., as $(1 - D/2w)^2$, when the cylinder is barely in the slush-overlap region. (As mentioned in the Introduction, in the original KKHB paper,[6] a linear behavior was hypothesized.) The reason is that the cylinder contribution to the hydrodynamic force is (cf. Eqs. 11 and 12),

$$F_H^{(c)} = \pi \int_0^{\sqrt{2R(2w-D)}} r^2 dr \frac{dP}{dr} \qquad . \qquad (28)$$

Since P is analytic at $r=0$, it must vary as $a+br^2+...$, at small r, where a and b are constants. Thus dP/dr is proportional to r, to leading order, and the integral of Eq. 28 to $(2w-D)^2$.

The explicit results obtained for the hydration force to this point refer to an obviously oversimplified model of the spatial variation of the viscosity, i.e., a step-function switchover from "slush" to "water" dissipation. For a general viscosity function, one can derive explicit asymptotic results, which may, in the end prove more valuable.

The first result concerns the behavior of the hydration force near D=0. In that limit, Eq. 16 becomes

$$F_H = -\frac{\pi}{2} \int_0^{\sqrt{4Rw}} dr \frac{r^3}{g(r)} \frac{dD}{dt} \qquad , \qquad (29)$$

where I retain the assumption that the slushy region has width w and drop the contribution from outside the corresponding pure slush cylinder. To evaluate $g(r)$, I rewrite Eq. 15, exactly, as

$$g(r) = 2D^3 \int_0^{\left(1+\frac{v^2}{2R}\right)/2} du \frac{\left(u - \left(1+\frac{v^2}{2R}\right)/2\right)^2}{\eta(Du)} \qquad , \qquad (30)$$

where $v \equiv r/D^{1/2}$. Note that in Eq. 30, there is no harm in setting D=0 in the argument of η, yielding the asymptotic result, upon substitution of Eq. 30 into Eq. 29,

$$F_H = -6\pi\eta(0) \frac{R^2}{D} \frac{dD}{dt} \qquad . \qquad (31)$$

The second general asymptotic result is for D slightly smaller than $2w$. In this limit, Eq. 16 becomes,

$$F_H = -\frac{\pi}{2} R^2 \frac{dD}{dt} \frac{1}{g(0)} (2w - D)^2 \qquad . \qquad (32)$$

To evaluate g at r=0, I start from Eq. 15 and easily derive,

$$g(0) = \frac{D^3}{4} \int_0^1 du \, \frac{(u-1)^2}{\eta(Du/2)} \qquad . \qquad (33)$$

This is as far as one gets for a general viscosity function. Eq. 33 does show, however, that if the viscosity approaches that of water gradually, instead of stepwise at the slush edge, then the quadratic dependence of the hydration force may be modified. For example, suppose the viscosity of water is zero, to a good approximation, and that the slush viscosity diminishes to zero linearly, according to

$$\eta(z) = \eta_s (1 - z/w) \qquad . \qquad (34)$$

Then the vanishing of the viscosity at $u=1$ in the integrand of Eq. 33 gives rise to a logarithmic singularity of $g(0)$ at $D=2w$. As a consequence, the hydration force varies as

$$F_H = -\frac{\pi}{2} \frac{R^2}{D} \frac{dD}{dt} \eta_s \left(\frac{2w}{D} - 1\right)^2 \frac{1}{\ln(2w/D - 1)} \qquad . \qquad (35)$$

This is an important result, not because data at present suggest the viscosity drops off linearly, but because it exemplifies the possibility that highly accurate measurements of F_H vs. D might reveal the detailed spatial dependence of the viscosity.

Comparison of drainage theory to KKHB's experiment – If the hydrodynamic, step-function interphase model is a faithful description of KKHB's IFM experiments,[6] then observed forces, F, versus separations, D, should lie on curves of the form (cf., Eq. 21),

$$F = \frac{av}{D-b(v)}\left(1-\frac{D-b(v)}{2w(v)}\right)^2 \quad , \qquad (36)$$

where a, $b(v)$, and $w(v)$ are fit parameters and v is the tip-sample approach speed.

According to Eq. 21, $a = 6\pi\eta_s R^2$, where R is the tip radius and η_s is the interphase viscosity. This is why I represent a as independent of tip speed in Eq. 36.

In contrast, I allow $b(v)$, the position where the force tends asymptotically to "infinity," to depend on v. This may seem surprising, given that in Fig. 2 (copied from Ref. 6) only one vertical asymptote is shown for the two approach speeds. Fig. 2 was drawn that way because "relative" displacement on its x-axis was meant to have been defined so that the displacements where the tip and sample first touch, would line up.[12] Close reexamination of the data, however, reveals that this goal was not quite achieved. Therefore, in revisiting the data of Ref. 6, I have allowed the vertical asymptotes, $b(v)$, to differ for the two tip speeds.

The interphase width, w, a static property of the near-surface water, should *not* be a function of tip speed in Eq. 36. Nonetheless, given that Ref. 6's measurements for the two tip speeds were performed over different regions of a presumably somewhat heterogeneous SAM, it is not inconceivable that different values of w would have emerged from the two measurements.[13] In any event, i.e., whatever the reason may be, further reexamination of Fig. 2 makes plain that the tip-sample separation where the force vanished was *not* the same for the two tip speeds. Accordingly, I have allowed w to be different for the two values of v.

The search for parameters that minimize the residual,

$$R = \sum_n \left\{ F_n(v) - \frac{av}{D_n - b(v)}\left(1 - \frac{D_n - b(v)}{2w(v)}\right)^2 \right\}^2 \quad , \qquad (37)$$

is relatively straightforward, as it is strongly constrained by the many data points KKHB reported for $v = 1.3$ nm/sec. Figs. 3 and 5 illustrate the quality of the fit corresponding to $a = 0.277$ μN-sec, $b(1.3$ nm/sec$) = 1.31$ nm, $b(7.3$ nm/sec$) = 0.45$ nm, $w(1.3$ nm/sec$) = 2.1$ nm, $w(7.3$ nm/sec$) = 4.1$ nm.

In Fig. 3, the force data are plotted directly against displacement, and the solid curves are drawn using the above parameters in Eq. 36. In Fig. 5, F is plotted versus $\dfrac{v}{D-b(v)}\left(1-\dfrac{D-b(v)}{2w(v)}\right)^2$. In this linear graph of the F vs. D relation, the equality of a for the two tip speeds is easy to appreciate.

The value of a derived from fitting, 0.277 μN-sec, together with the known tip radius, R=0.5μm, yields the corrected, measured interphase viscosity, 59 KPa-sec. This is 6.6×10^7 greater than the viscosity of bulk water[11] (and 33 times larger than the result initially reported in Ref. 6).

Given that the interphase widths measured at two different tip speeds, $w(v)$, were not equal, but rather 2.1 and 4.1 nm for $v = 1.3$ and 7.3 nm/sec, it is reasonable to view the final numerical results with a certain skepticism. The difference of 2.0 nm in the interphase widths for the two speeds is anything but small compared to the absolute values. We can confidently conclude that the interphase width is a few nm and its viscosity is 10^7 - 10^8 times that of bulk water. Beyond that, the analysis makes clear that more data from better-characterized surfaces are needed.

Summary –
In the lubrication approximation, the Navier-Stokes equations are susceptible to a simple solution for the force that resists tip-sample approach, even if the viscosity is a spatially-varying quantity. If the interphases on the tip (of curvature radius R) and sample surfaces can be described as regions of a given width, w, wherein the viscosity, η_s, is constant and much higher than in bulk water, then the necessary quadratures can be performed explicitly, and the force vs. separation curve is given by Eq. 21,

$$F_H{}^{(c)} = -6\pi\eta_s \frac{R^2}{D}\frac{dD}{dt}\left(1-\frac{D}{2w}\right)^2 \quad . \qquad (21)$$

Even if the viscosity variation is more complicated, indeed, even if its variation is not known, the force near zero separation can be specified. It is given by Eq. 31,

$$F_H = -6\pi\eta(D=0)\frac{R^2}{D}\frac{dD}{dt} \qquad . \qquad (31)$$

KKHB's measurements for two different approach speeds obey these equations at small separations, *D*, but with somewhat different values of *w*. One may hope that further experiment will eliminate this discrepancy, perhaps through averaging over surface inhomogeneities. The Navier-Stokes solution presented here implies that a force vs. separation measurement can provide information on the spatial variation of the viscosity, in principle. This result stands as a further invitation to try to acquire the highest quality data.

(1) Vogler, E. A, *Adv. Colloid Interface Sci*. **1998**, 74, 69.

(2) Israelachvili, J., *Intermolecular and Surface Forces*, Academic Press: London, 1992.

(3) Schwendel, D.; Hayashi, T.; Dahint, R.; Pertsin, A.; Grunze, M.; Steitz, R.;

Schreiber, F., *Langmuir* **2003,** *19,* 2284.

(4) Zhu, Y.; Granick, S., *Phys. Rev. Lett*. **2001**, 87, 096104.

(5) Raviv, U., Laurat, P.; Klein, J., *Nature*, **2001**, 413, 52.

(6) Kim, H. I.; Kushmerick, J. G.; Houston, J. E.; Bunker, B. C., *Langmuir*, **2003,** *19,* 9271.

(7) Joyce, S. A.; Houston, J. E., *Rev. Sci. Instrum*. **1991**, 62, 710.

(8) Chan, D. Y. C.; Horn, R. G., *J. Chem. Phys*. **1985**, 83, 5311, Appendix A

(9) Reynolds, O., Philos. Trans. R. Soc., London **1886**, 177, 157.

(10) Tichy, J. A., *Tribology Transactions* **1995**, 38, 577.

(11) Lide, D. R., Ed., CRC Handbook of Chemistry and Physics; 79 ed.; CRC Press: Boca Raton, **1998**.

(12) Houston, J. E., private communication.

(13) A natural-seeming explanation of why w should depend on v (Held, G., and independently Bunker, B. C., private communication), namely that drainage pressure under the tip might cause interphase restructuring and, specifically, a speed-dependent interphase width, is unfortunately not viable. The trouble with this idea is that pressure in the fluid rises only *after* tip and sample interphases make contact. Before that, drainage is rapid and the pressure is constant and low.
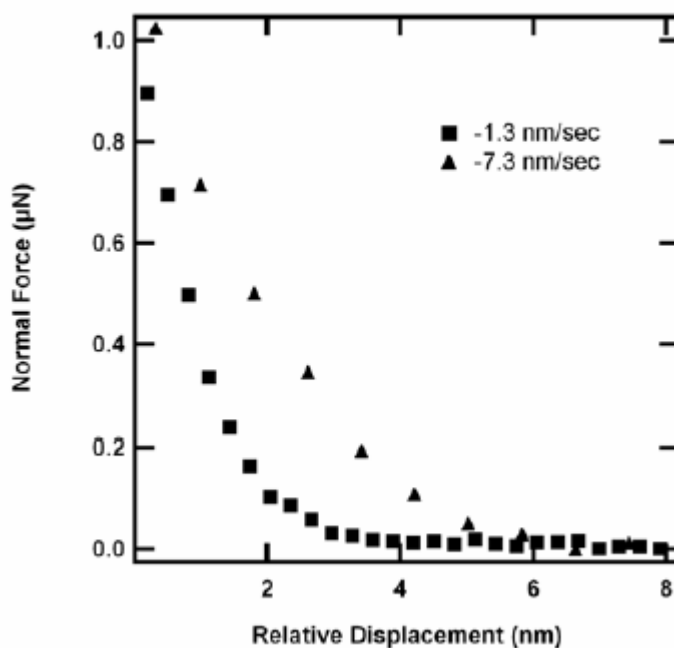
Fig. 1 – After Ref. 6, for a gold tip and sample in water, each functionalized by an $HS(CH_2)_{11}(OCH_2-CH_2)_3OH$ self-assembled monolayer, the normal force on the tip as a function of its velocity, as measured using an IFM
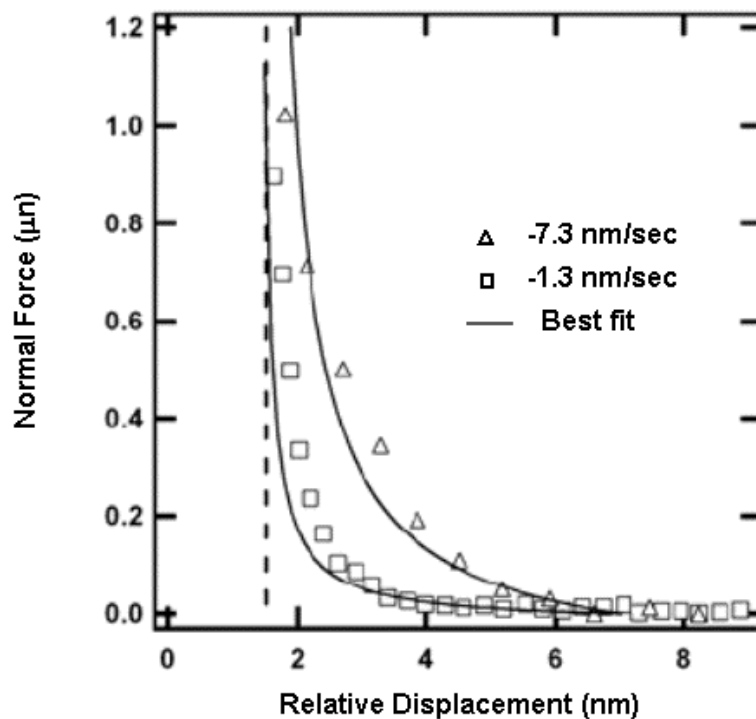

Fig. 2 – After Ref. 6, for a gold tip and sample in water, each functionalized by an $HS(CH_2)_{11}(OCH_2-CH_2)_3OH$ self-assembled monolayer, data points representing the normal force on the tip as a function of its velocity, as measured using an IFM and corrected for the compliances of the SAM's and of the Au tip and sample, and lines indicating fits of $6\pi\eta R^2 v(1/D - 1/D_0)$ to the data.
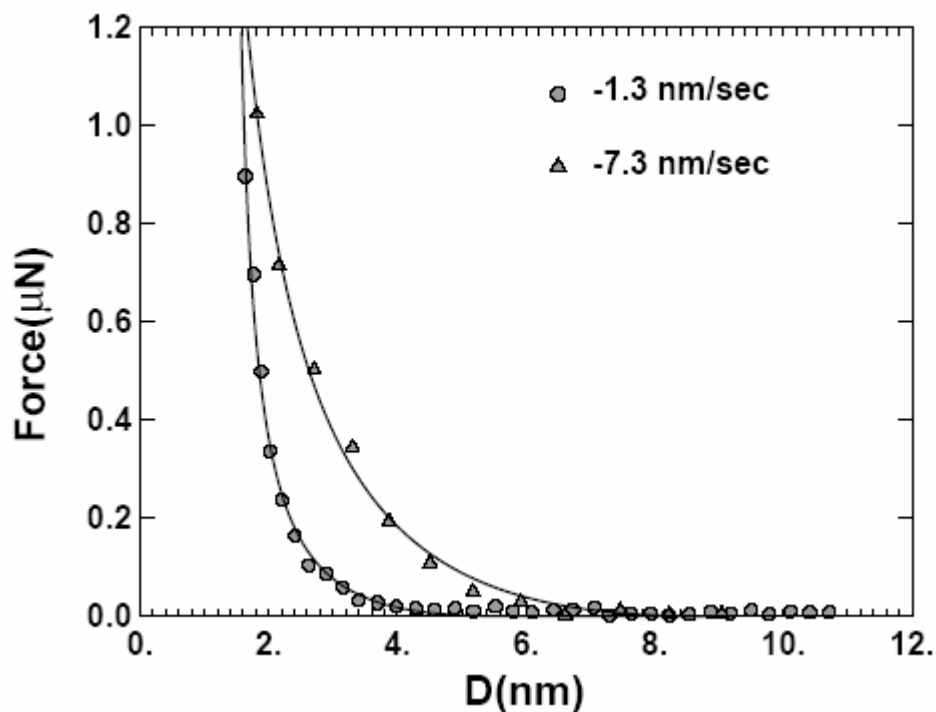
Fig. 3 – For a gold tip and sample in water, each functionalized by an $HS(CH_2)_{11}(OCH_2$-$CH_2)_3OH$ self-assembled monolayer, data points representing the normal force on the tip as a function of its velocity, as measured using an IFM and corrected for the compliances of the SAM's and of the Au tip and sample, and lines indicating fits of the force formula derived here [see Eq. 21] to the data. "D" is the "relative displacement" as in Fig. 2.
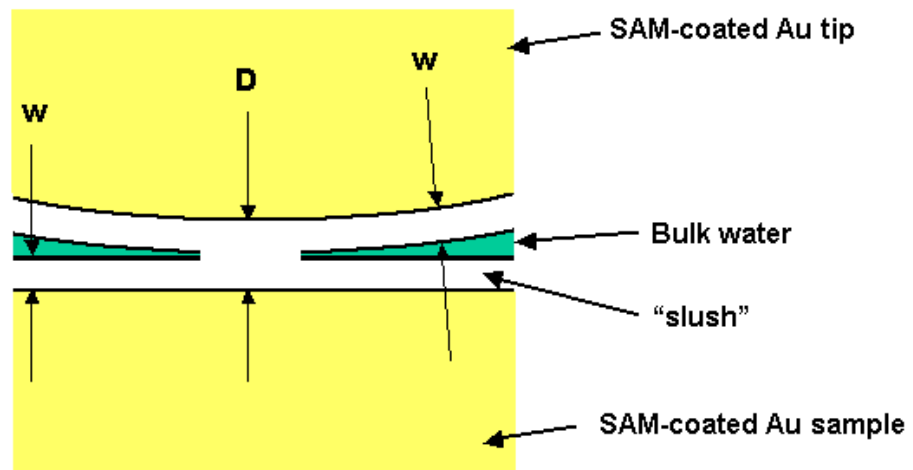
Fig. 4 - When the tip apex is within *2w* of the planar sample surface, the *interphase* or "slush" regions associated with the two surfaces overlap, giving rise to unusually large dissipative forces.
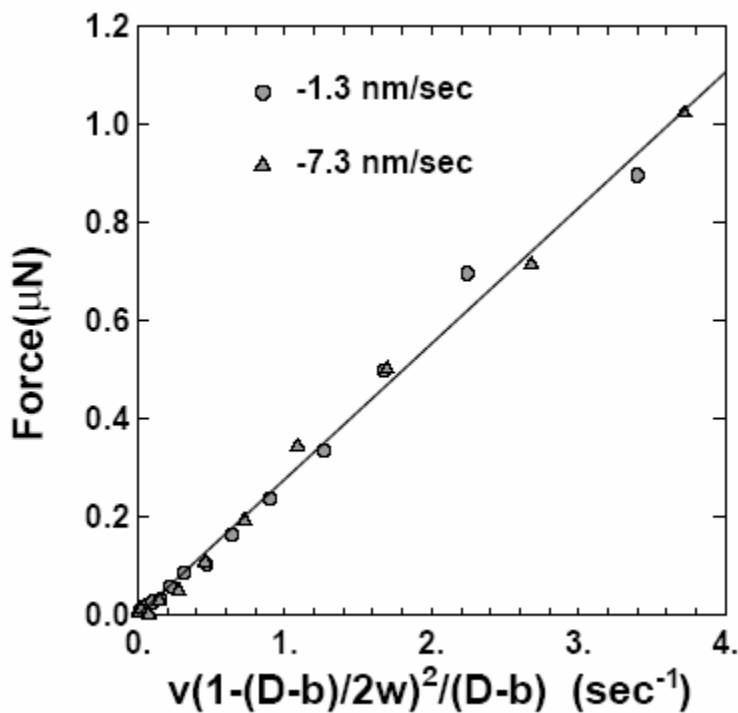
Fig. 5 – For a gold tip and sample in water, each functionalized by an EG3OH self-assembled monolayer, the corrected normal force vs. separation and velocity data of Fig. 3, replotted with the x-axis rescaled according to Eq. 21. The linearity of the data, after this rescaling, shows that Eq. 21 is a good representation of the measured force versus tip-sample separation and approach speed. For the data corresponding to tip velocity –1.3 nm/sec, the rescaling of the x-axis was done with b=1.31 nm and w=2.1 nm. For the data taken at –7.3 nm/sec, I used b=0.45 nm and w=4.1 nm. The slope of the solid line is 0.277 μN-sec.

Distribution

1 MS 0123   Donna L. Chavez, LDRD Office, 01011

1 MS 1413   Bruce C. Bunker, 1116

1 MS 1413   Kevin Leung, 1116

1 MS 1415   Jack Houston, 1114

1 MS 1415   Peter J. Feibelman, 1114

1 MS 1415   Neal D. Shinn, 1114

1 MS 1421   Dale L. Huber, 1112

1 MS 1427   Julia M. Phillips, 1100

1 MS 0619   Creative Arts Department, 12620

1 MS 9018   Central Technical Files, 8945-1

2 MS 0899   Technical Library, 9616